A two-layer energy management system for a hybrid electrical passenger ship with multi-PEM fuel cell stack

Xie, Peilin; Asgharian, Hossein; Guerrero, Josep M.; Vasquez, Juan C.; Araya, Samuel Simon; Liso, Vincenzo

Published in:
International Journal of Hydrogen Energy

DOI (link to publication from Publisher):
10.1016/j.ijhydene.2023.09.297

Publication date:
2024

Document Version
Publisher's PDF, also known as Version of record

Available online at www.sciencedirect.com

ScienceDirect

journal homepage: www.elsevier.com/locate/he

A two-layer energy management system for a hybrid electrical passenger ship with multi-PEM fuel cell stack

Peilin Xie[*], *Hossein Asgharian, Josep M. Guerrero, Juan C. Vasquez, Samuel Simon Araya, Vincenzo Liso*

AAU Energy, Aalborg University, Aalborg, 9220, Denmark

HIGHLIGHTS

- Hybrid PEM fuel cell/battery system enables zero-emission shipping.
- Two-layer EMS enhances fuel efficiency while satisfying real-time load requirements.
- Rotational sequential distribution prevents uneven degradation.
- Rotational sequential distribution enhances computational efficiency.

GRAPHICAL ABSTRACT

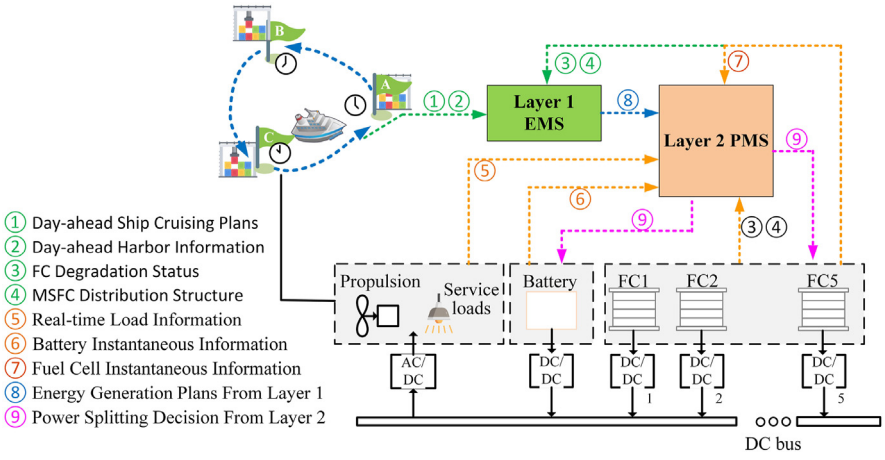

ARTICLE INFO

Article history:
Received 28 June 2023
Received in revised form
22 September 2023
Accepted 28 September 2023
Available online 14 October 2023

Keywords:
Energy management
Fuel cell
PEM
Shipboard microgrid

ABSTRACT

The hybrid combination of hydrogen fuel cells (FCs) and batteries has emerged as a promising solution for efficient and eco-friendly power supply in maritime applications. Yet, ensuring high-quality and cost-effective energy supply presents challenges. Addressing these goals requires effective coordination among multiple FC stacks, batteries, and cold-ironing. Although there has been previous work focusing it, the unique maritime load characteristics, variable cruise plans, and diverse fuel cell system architectures introduce additional complexities and therefore worth to be further studied. Motivated by it, a two-layer energy management system (EMS) is presented in this paper to enhance shipping fuel efficiency. The first layer of the EMS, executed offline, optimizes day-ahead power generation plans based on the vessel's next-day cruises. To further enhance the EMS's effectiveness in dynamic real-time situations, the second layer, conducted online, dynamically adjusts power splitting decisions based on the output from the first layer and

* Corresponding author.
E-mail address: pxi@energy.aau.dk (P. Xie).

https://doi.org/10.1016/j.ijhydene.2023.09.297

instantaneous load information. This dual-layer approach optimally exploits the maritime environment and the fuel cell features. The presented method provides valuable utility in the development of control strategies for hybrid powertrains, thereby enabling the optimization of power generation plans and dynamic adjustment of power splitting decisions in response to load variations. Through comprehensive case studies, the effectiveness of the proposed EMS is evaluated, thereby showcasing its ability to improve system performance, enhance fuel efficiency (potential fuel savings of up to 28%), and support sustainable maritime operations.

Nomenclature

ΔP_{fc}	Allowed FC output power variation from the reference value, kW
$\dot{C}_{bat}$	Equivalent instantaneous fuel consumption rate of battery, kg/h
$\dot{C}_{fc,i}$	Instantaneous fuel consumption rate of ith FC, kg/h
$\dot{C}_{fc,tot}$	Total fuel consumption rate of the MFCS system, kg/h
$\eta_{chg.av}$, $\eta_{dis.av}$	Average charging and discharging efficiency of battery
$\eta_{fc,i,t}$	Efficiency of ith FC at time t
$\eta_{fc,i}$	Efficiency of i^{th}FC
$\eta_{fc,tot}$	Total efficiency of the MFCS system
$\eta_{fc.av}$	Average FC efficiency
ef_{bat}	Battery equivalence factor
I_{bat}	Battery current, A
$k_{fc,i,t}$	On/off of ith FC at time t
N_{fc}	Total number of FC stacks
$P_{bat(min)}$, $P_{bat(max)}$	Lower and upper limits of the battery output power, kW
P_{bat}	Output power of battery, kW
$P_{ci,t}$	Cold-ironing power at time t, kW
$P_{fc(min)}$, $P_{fc(max)}$	Lower and upper limits of the FC output power, kW
$P_{fc,i,ref}$	Reference ith FC output value from the first layer, kW
$P_{fc,i,t}$	Output power of ith FC at time t, kW
$P_{fc,i}$	Output power of i^{th}FC, kW
$P_{fc,tot}$	Total output power of the MFCS system, kW
$P_{load,t}$	Load demand at time t, kW
$P_{loss_{bat}}$	Battery power losses, kW
$P_{tot,ref}$	Hourly MFCS output power from the first-layer EMS, kW
Q_{bat}	Battery capacity, Ah
R_{bat}	Battery internal resistance, Ω
$SOC_{bat(min)}$, $SOC_{bat(max)}$	Lower and upper limits of the battery SOC
SOC_{bat}	Battery SOC
SOC_{desire}	Desired SOC level
T_s	FC power time constant, s
$u_{fc,i}$	Reference output power of i^{th}FC, kW
$u_{fc,tot}$	Reference output power of MFCS, kW
V_{oc}	Open-circuit voltage of the battery, V
BoL	Beginning of life
ECMS	Equivalent consumption minimization strategy
ESS	Energy storage systems
FC	Fuel cell
MFCS	Multi-fuel cell stack
PEM	Proton exchange membrane
SFC	Specific fuel consumption
SPS	Shipboard power systems

1. Introduction

Stringent ambitions have been proposed by the International Maritime Organization for the maritime transportation to reduce the green house gas emission by 40% by 2030 and 70% by 2050 compared with 2008 level [1]. However, traditional fossil fuels are still the major power source for over 95% of ships [2]. Motivated by the decarbonization goals, hydrogen is considered to be an emission-free energy source and thereby attracting increasing interests.

Proton exchange membrane (PEM) fuel cell is a strong candidate to provide major power supply for the future maritime application due to the advantages of quick start-up, high efficiency, and low operating temperatures [3]. However, PEM fuel cell has a relatively long start-up time of up to 30 min, and its dynamic response to load fluctuations is slow [4,5]. To guarantee the reliability of power supply when applying PEM FC on ships, batteries are often used as auxiliary in compensation for the slow dynamic response of the FC. The hybrid use of these energy sources provides opportunities for more efficient operation but relies heavily on their cooperation as well. Furthermore, considering the fact that a single PEM FC stack can hardly meet the heavy maritime load demand, a multi-fuel cell stack (MFCS) system is an alternative option that offers more freedom of operation but further complicates the electrical system [6]. Therefore, an energy management

system is essential to ensure the operational efficiency for such multi-energy microgrid.

While PMSs have seen substantial development across various applications such as terrestrial [7], residential [8], vehicle [9], and aircraft power systems [10], shipboard microgrids present unique challenges and specific demands. A primary distinction is that the shipboard microgrid can be treated as a mobile microgrid [11] and the propulsion loads takes a significant proportion of onboard loads. Consequently, the onboard load profile exhibits distinct patterns based on different cruising plans, further influenced by environmental factors such as wind and sea waves [12]. Cruising plans are often relatively fixed or readily obtained beforehand, enabling similar load curve trends in specific voyages for easy statistical analysis and forecasting. However, during real-time navigation, propulsion loads can experience severe fluctuations due to ventilation, shifts in shipping modes, and ship in-and-out-of water effects [13]. These dynamics pose considerable challenges for accurate load predictions and continuous power maintaining.

Given the different characteristics of the onboard loads under long-term time horizon and short-term time horizon, the existing EMSs for shipboard microgrids generally handle these aspects independently and therefore can be categorized into two parts, "early-stage energy dispatching" and "real-time power allocation".

"Early-stage energy dispatching" requires a prior knowledge of the shipping load profile, and is always strongly coupled with the facility sizing problem. Based on the historical load database or predicted values, the energy dispatching plans can either be obtained by optimization-based methods [14–17] or rule-based methods [18–20]. For example in Ref. [21], an optimization problem is formulated based on the specific fuel consumption (SFC) curve of FC to minimize the fuel consumption. Additionally [22], incorporates cold-ironing power and determines the energy dispatching plan with the aim of minimizing the ship daily operation cost. Moreover [23], takes into consideration not only the investment cost, but also factors such as fuel consumption, personnel electrical safety, and occupied volume of the SPS. It is worth noting that such optimization problems often lead to an overwhelming number of variables and constraints that pose computational challenges. One potential solution is the application of advanced algorithms. For example in Ref. [24], an iterative blackbox optimization algorithm is employed to address the optimal sizing problem. Additionally, in Ref. [25], a combination of quantum computing mechanism and swarm intelligence algorithm is utilized to efficiently tackle the multi-objective optimization problem with rapid convergence and strong robustness. Another approach to managing the computational burden of heavy optimization is to implement a multi-layer hierarchically structured architecture, which involves breaking down a single optimization problem into several hierarchical sub-problems. For example in Ref. [26], a bilevel optimization framework is introduced. This framework optimizes the fuel cell and battery size on the upper layer, while handling generation and voyage scheduling in the lower layer.

For the purpose of enhancing computational efficiency, certain studies make a trade-off between optimality of results. They employ rule-based methods to derive the power distribution plan by adhering to a set of predefined rules. Following this, optimization-based algorithm is employed to determine the optimal sizing of the onboard facilities. For example in literature [27,28], support vector machines are adopted to control the power flow between the fuel cell and the hybrid energy storage systems, after which the optimal sizing of the onboard facilities are determined. Such methods compromise for the power distribution efficiency, but can largely reduce the computational effort especially when there are multiple or conflicting optimization objectives such as minimization of greenhouse gas emission, total cost or footprints. To conclude the existing work on "early-stage energy dispatching", they contribute to the high efficient shipping and optimal facility sizing by making energy generation plans ahead of time. However, the results are mostly obtained from a long-term perspective and pre-defined load profiles, thus not suitable for the real-time applications due to the high dynamics and variation of onboard loads.

To better adapt to highly dynamic conditions and ensure fuel efficient operations while satisfying the instantaneous load demands, research efforts have been focused on "real-time power allocation". In these studies, no prior knowledge of the shipping information is required, and power splitting decisions are made based only on real-time updated load information. Commonly used methods are filter-based methods [27,29], PI-based methods [30], rule-based methods [31], optimization-based methods [32–36], and artificial intelligence (AI)-based methods [37,38]. For example, in Ref. [39], a PI-based EMS is proposed, utilizing a hybrid metaheuristic optimization technique called JSPSOBAT tp determine optimal PI gains. In Ref. [40], Finite State Machines are employed to coordinate the behavior of fuel cells and the battery, enabling seamless transitions between black start, normal, transient, and faulty states. Additionally [41], introduces a fuzzy controller based on the Whale Optimization Algorithm to effectively reduce hydrogen consumption. Furthermore, in Refs. [42,43], the particle swarm algorithm is applied to address optimization problems with the goal of achieving enhanced power quality. Among these papers, it is noteworthy that while the first three categories are simple in structure, their performance heavily relies on engineering experience and may not ensure the attainment of optimal solutions [44]. And although the AI-based and optimization-based methods are considered to be able to obtain the optimum operating point, they can be time-consuming, thus increasing the complexity for real-time execution. Moreover, since only instantaneous situations are considered for real-time optimizations, there is no guarantee that the obtained results are globally optimal, even with advanced methods.

After reviewing the current efforts on the development of onboard energy management systems, it can be found that trade-offs are often inevitable, either in system dynamics or less-than-optimal outcomes. Considering the unique characteristics of the onboard loads: long-term regularity and short-term unpredictability, both aspects play pivotal roles in optimizing power sharing decisions. This forms the core focus of this paper. In our previous paper [45], a day-ahead EMS is proposed to optimize the power generation plans based on next-day cruising requirements. However, the dynamic

nature of real-time power demands remained a challenge. The onboard loads would vary greatly with different ship cruising plans and would be highly fluctuated due to changeable sea waves and real-time sailing conditions. Although it is possible to predict the general load profile over a longer time period by analyzing the ship's future cruise plan, it is difficult to accurately predict the loads in real-time due to their high volatility. As a result, achieving fuel-efficient operation with a globally optimal approach while satisfying instantaneous fluctuating load demand is still a significant challenge and is the major focus of this paper.

In this paper, we extend the EMS by proposing a two-layer scheme that takes in to account the onboard load characteristics. The outer layer takes full use of the predictable nature of propulsion load over an extended period and therefore enables the system to make informed decisions for more fuel-efficient operation. Simultaneously, the inner layer considers the inherent volatility of the instantaneous load fluctuations and enables real-time power splitting to meet the dynamic demands efficiently.

In addition to the challenges brought by propulsion load, another research gap for the existing studies is that most of them are designed for single FC systems and only a few address the EMS design for the multi-fuel cell stack system. There are currently three basic power distribution strategies for MFCS system: equal distribution, sequential (or Daisy chain) distribution, and independent (or optimal) distribution [46]. Comparisons have been conducted between the three types [47,48] and efforts have been made to improve their fuel efficiency [46,49,50], equaling their degradation levels [51,52], or guarantees the SOC consensus of storage systems [53]. Estimating the degrading status of each FC stack and allocating the load according to their specific efficiency operational points is a common method which has proven to be effective in extending the MFCS life time [51]. However, most of the current studies are conducted based on specific types of loads and neglect the peculiarities of onboard loads (high variability, large fluctuations, long-term regularity and short-term unpredictability). Therefore, the effectiveness of the existing EMS is subject to further discussion when applied to maritime applications.

To address all the above challenges, this paper proposes a two-layer EMS for a hybrid MFCS/battery passenger ship and compares it with several most commonly adopted methods to test its effectiveness. The first layer EMS is built in GAMS and solved by BONMINH, and the second layer is conducted on MATLAB/Simulink 2022a. The two-layer EMS is developed from different time scales with two objectives: (i) enabling high fuel-efficiency operation, and (ii) healthy battery SOC level, throughout the one-day cruising. The contributions of this paper are summarized below:

1. A novel two-layer EMS is developed which consists of a day-ahead offline optimization layer and a real-time online power management layer. The proposed EMS takes full advantages of the long-term perspective of global optimization and the fast executing speed of the rule-based method to realize near-global optimal solutions with less computational effort and thus suitable for real-time application.
2. The proposed EMS is developed with respects to the specific characteristics for the three MFCS distributions to improve the overall fuel efficiency of the MFCS. In addition, the degradation status of each FC is considered and a special rotational sequential mode is designed to avoid the usage of severely degraded FCs and thereby improving operating efficiency.
3. The proposed EMS is simple in structure and is able to provide customized power generation plans based on different cruises, MFCS distributions, and FC degradation states, and therefore can be easily applied to other marine applications as well.

This paper is organized as follows. In Section 2, the ship structure is described and the electrical components are modeled. The proposed EMS is presented in Section 3. The case studies are investigated and discussed in Section 4. Conclusion is given in Section 5 and full simulation results under different cases are presented in Appendix.

2. System description and modeling

The ship studied in this paper is a passenger ship that transfers travelers between three harbors every day. The ship can be seen as a mobile microgrid that works in islanded mode when at sea and in grid-connected mode when at the ports. The majority of the power onboard the ship is supplied by 5 fuel cell stacks, and a battery provides auxiliary support for the onboard loads. When the ship arrives at the harbor, it gets access to the “cold ironing”. There are mainly two types of onboard loads, namely propulsion load and service load. The propulsion load accounts for the majority of the onboard load during the voyage and is largely affected by the ship cruising routine and speeds. The service load is much lower than the propulsion load but is the main load at berth. The hourly load profile can be easily obtained by the next-day ship cruising plans and the historical load profile. And the adopted load profiles in this paper are obtained from Refs. [54,55]. However, due to the presence of variable sea conditions, cruising modes, and customer requirements, the real-time onboard loads will fluctuate and deviate from pre-assumed values. These fluctuations are hard to predict ahead of time and therefore modeled by random stepping load changes. The modeling of each electrical component is given in the following subsections.

2.1. *Fuel cell*

2.1.1. *PEM fuel cell model*

In this subsection, the mathematical models of PEM fuel cell in terms of pressure drop, compressor power consumption, and degradation are investigated.

The pressure drop on the anode side is much lower than that on the cathode side, and the hydrogen is always pressurized in the tank before it is used on the anode side [56]. Therefore, the pressure drop on the anode side is ignored in this paper, and only the pressure drop on the cathode side is considered and is calculated by the sum of major pressure loss and minor pressure loss using the following equation [57]:

$$\Delta P = \int_0^L \frac{f\rho}{2d} V^2 dx + \sum_1^i k \frac{\rho}{2} V^2 \quad (1)$$

where f represents friction coefficient, ρ, L, k, d, i are constant values representing air density, channel length, minor loss coefficient, channel hydraulic diameter, and the number of swerve corners in gas channels, respectively. V is the gas flow rate, and it varies with load changes. The velocity of air which enters each cell in the stack is given as follows:

$$V = \frac{\dot{m}_{air} S}{\rho A n} \quad (2)$$

where n, S, and A represent the number of cells in each stack, stoichiometry, and gas channel cross section area, respectively. $\dot{m}_{air}$ stands for the air mass flow rate that enters each cell and is given as follows:

$$\dot{m}_{air} = \frac{M_{air} P}{0.21 \times 4 \times V_c F} \quad (3)$$

where M_{air}, P, F, and V_c represent the molar mass of air, fuel cell power, cell voltage, and Faraday number, respectively. As mentioned before, the air mass flow rate, and consequently the velocity in gas channels is not constant since the oxygen content of air is consumed. Considering the mass flow rate variation, the gas channels are discretized into cells and a constant source term is imposed to each cell to account for the oxygen consumption. As a result, the mass flow rate of air which leaves each gas channel can be calculated as follows:

$$\dot{m}_{air.out} = (3.57S \times 10^{-7} - 8.29 \times 10^{-8}) \frac{P}{V_c} \quad (4)$$

The friction coefficient f in equation (1) for air laminar flow can also be calculated as follows:

$$f = \frac{64}{Re} \quad (5)$$

where Re is the Reynolds number and can be calculated by

$$Re = \rho V d / \mu \quad (6)$$

μ is the dynamic viscosity in kg/(m• s).

The model for calculation of pressure drop in the fuel cell stack is validated using the data given in Ref. [58]. The conditions discussed in the reference are used to calculate the pressure drop for a wide range of power. Fig. 1 compares the value of pressure drop calculated using the model and the data given by the reference, and the results validate the effectiveness of the developed model.

Once the pressure drop in the gas channels and manifolds of the fuel cell stack is calculated, the power required in an isentropic compression process to compensate for the pressure drop can be calculated as follows [59]:

$$P_{is} = 2310 \times \frac{k(T_{dis} - T_{suct})}{(k-1)M} Q \quad (7)$$

where T_{suct}, Q, and M represent compressor inlet temperature, gas mass flow rate, molar weight of gas, respectively. k denotes air isentropic constant with value of 1.4. T_{dis} is compressor outlet temperature and can be calculated as follows for an isentropic compression process:

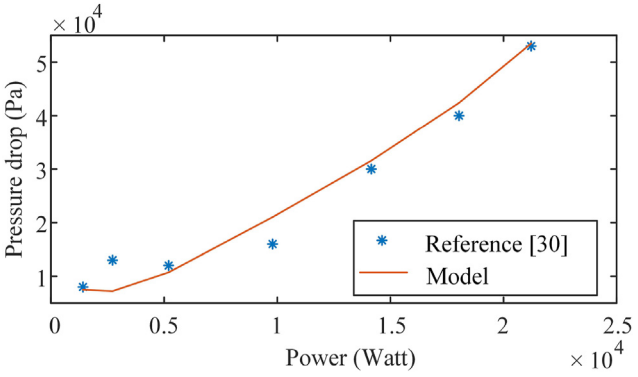

Fig. 1 – Comparison of the developed model for the effect of inlet air pressure drop on power losses in the PEMFC operations (data obtained from Ref. [58]).

$$\frac{T_{dis}}{T_{suct}} = \left(\frac{P_2}{P_1}\right)^{\frac{\gamma-1}{\gamma}} \quad (8)$$

where P_2 and P_1 represent the compressor inlet and outlet pressure, while γ is heat capacity ratio which is given as follows:

$$\gamma = \frac{C_p}{C_V} \quad (9)$$

It is worth noting that in this study nonidealities in the compression process are taken into account using isentropic efficiency. As a result, the actual required power in the compressor can be calculated as follows:

$$P_{act} = \frac{P_{is}}{\eta} \quad (10)$$

where η is isentropic efficiency of the compressor. The efficiency of the fuel cell stack can also be calculated as follows:

$$\eta_{fc} = \frac{P_{fc}}{\dot{m}_{H_2} LHV_{fuel}} \quad (11)$$

where LHV_{fuel} represents the lower heating value of hydrogen, and is set as 33.33 kWh/kg, P_{fc} and $\dot{m}_{H_2}$ are the net power output of the fuel cell stack and hydrogen mass flow rate which enters the anode, respectively. These two parameters can be calculated as follows:

$$P_{fc} = P - P_{act.compressor} - 0.03 \times P \quad (12)$$

$$\dot{m}_{H_2} = 1.05 \times 10^{-8} \frac{P}{V_c} \quad (13)$$

As can be seen, to calculate the net output power of the fuel cell, in addition to the power consumption in the compressor, 3% of the total fuel cell power is also allocated to the parasitic load in auxiliary equipment.

Due to the degradation of fuel cell stack, the voltage is affected directly and can be calculated as follows according to Ref. [60]:

$$V_c = V_0 - (V_1' \times n_1 + U_1' \times t_1 + V_2' \times n_2 + U_2' \times t_2) \quad (14)$$

where V_0 is the voltage when the fuel cell is at beginning of life (BoL). V_1', U_1', V_2', and U_2' denote voltage degradation rates for start-stop cycles, idling period, load change cycle, and high-power load period, respectively. n_1, t_1, n_2, and t_2 represent the corresponding number of cycles and operational time, respectively.

To reduce the computational burden, the fuel cell performance is described in a lookup table based on the above mentioned mathematical models, as in Fig. 2. The curve fitted values are also presented. Results under different degradation status are presented, including undegraded (BoL), after 10 k hours of operation, after 20 k hours of operation, and after 30 k hours of operation. Fig. 2 indicates that the degradation results in a reduced fuel cell efficiency due to the power reduction of fuel cell and the increased power consumption in the compressor. According to equations (3) and (13), when the cell voltage decays due to degradation, the mass flow rates of air into the cathode and hydrogen into the anode increase. Referring to equations (11) and (12), when the net power output of the fuel cell stack decreases, due to voltage degradation and increase in power consumption of the compressor, this causes the efficiency of the fuel cell to decrease.

2.1.2. *Multi-fuel cell stack system model*

In this study, three types of power distributions are considered and listed below:

1. Equal distribution: the power demand is equally allocated to each module.
2. Independent distribution: the on/off status and output power of each FC can be controlled independently and is decided by the optimization algorithm.
3. Sequential distribution: the power demand is allocated to one module after another, where one module is activated when the previous one has reached maximum power output. This configuration is also known as "daisy-chain" power distribution.
4. Rotational sequential distribution: the uneven usage of FCs leads to different degradation status of FCs, and the difference would be more severe in sequential distribution since the first FC in the sequence is the most frequently used. In order to guarantee a similar degradation rate for all FCs, a sequence rotation procedure is developed by monitoring the degradation status of each FC and rearranging the sequence. In this way, all five FCs would have a similar degradation rate.

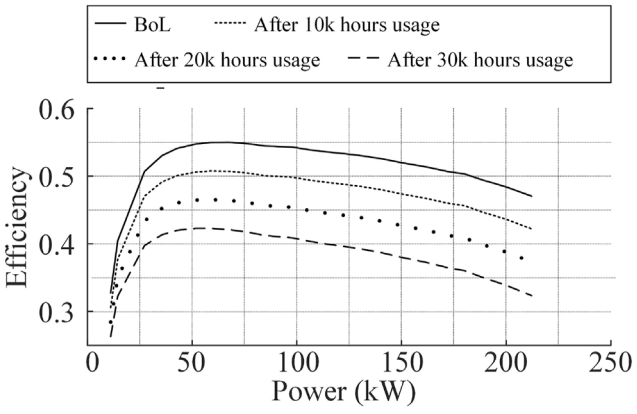

Fig. 2 – Fuel cell module efficiency curves under different degradation level.

In Fig. 3, the four different module load distribution configurations are shown. A power limiter between 15 and 200 kW was considered for each fuel cell module.

According to the mathematical model of single PEM FC stack, the total efficiency of the multi-fuel cell stack system can be obtained by the following equation:

$$\eta_{fc,tot} = \frac{P_{fc,tot}}{\dot{C}_{fc,tot} LHV_{fuel}} \quad (15)$$

$$\dot{C}_{fc,tot} = \sum_{i=1}^{N_{fc}} \frac{P_{fc,i}}{\eta_{fc,i} LHV_{fuel}} \quad (16)$$

where N_{fc} is the total number of FC stacks, $\dot{C}_{fc,tot}$ is the total fuel consumption rate of MFCS system, and $P_{fc,tot}$ is the total output power of the MFCS and is calculated by the sum of each FC stack output power. Due to the different ways of power distribution between the MFCS system, the overall fuel efficiency shows different characteristics, and therefore, the scheduling of the energy dispatching shall be made accordingly to improve the overall system fuel efficiency.

Considering the slow dynamics of fuel cell modules, it takes time for the FC output power to reach the reference value. To mimic the slow dynamics, the relationship between the reference power ($u_{fc,i}$) and the actual output power ($P_{fc,i}$) is expressed as:

$$P_{fc,i} = \frac{1}{T_s s + 1} u_{fc,i} \quad (17)$$

In the equation, T_s is the FC power time constant, and is set as 80s, and it stands for the time needed for the load step response to reach 63.2% of its final value. For FCs in independent distribution, there would be five control variables $u_{fc,1}$, $u_{fc,2}$, …, $u_{fc,5}$. They are the reference power for each fuel cell module. While for those in equal distribution and sequential distribution, all the fuel cells are treated as a whole and one control variable ($u_{fc,tot}$) would be enough, which stands for the total amount of FC reference power. The relationship between the overall reference variable ($u_{fc,tot}$) and actual output power ($P_{fc,tot}$) are the same:

$$\frac{dP_{fc,tot}}{dt} = -\frac{1}{T_s} P_{fc,tot} + \frac{1}{T_s} u_{fc,tot} \quad (18)$$

2.2. *Battery*

To compensate for the slow dynamic nature of hydrogen fuel cells, batteries are used to provide auxiliary support for the variable onboard load and to help keep the fuel cell in the high efficiency operation range. Since the main focus of this paper is on the application of fuel cells, the degradation of the battery is neglected to simplify the analysis. A generic battery model has been chosen and is presented below,

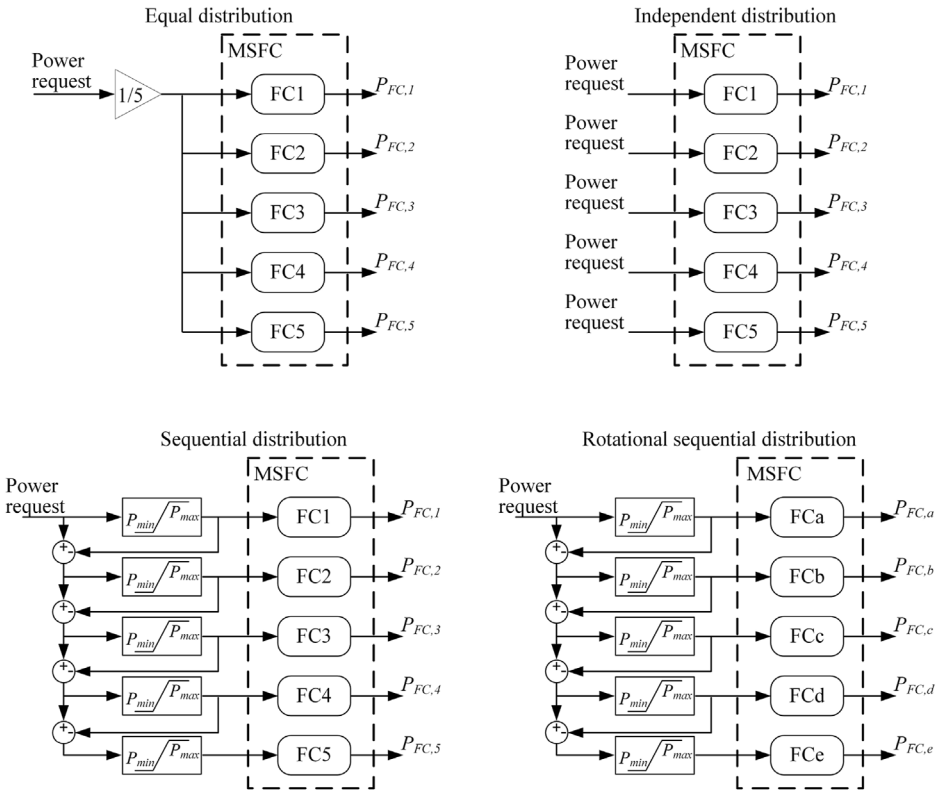

Fig. 3 – Four different types of power distribution among five fuel cell modules.

$$\dot{SOC}_{bat} = -\frac{1}{3600Q_{bat}} I_{bat} \tag{19}$$

where SOC_{bat} is the battery SOC, I_{bat} is the battery current, and Q_{bat} is the battery capacity. Taking the power losses into account, the output power of the battery (P_{bat}) can be expressed as follows,

$$P_{bat} = V_{oc} I_{bat} - P_{loss_{bat}} = V_{oc} I_{bat} - R_{bat} I_{bat}^2 \tag{20}$$

where V_{oc} is the open-circuit voltage of the battery, $P_{loss_{bat}}$ is the power losses caused by battery internal resistance R_{bat}.

The consideration of battery degradation was not included in this study. This decision was made based on the system configuration, which consists of a single battery for the entire system. Therefore, the results obtained would not be significantly affected by battery degradation.

3. Method

3.1. *Proposed two-layer energy management strategy*

In this paper, a novel two-layer energy management strategy is developed to acquire a highly fuel-efficient operation and maintain a secure SOC level of ESS. An overall structure of the proposed EMS is shown in Fig. 4.

The first layer is optimization-based, using the next-day load profile to make the day ahead energy dispatching plan, including the on/off status and reference output power values for each FC stack and battery. With this optimized energy dispatching plan, the second layer splits the real-time loads between the multiple energy sources to achieve reliable power supply and high fuel-efficiency operation. During this process, the changes of cruising plans, availability of cold-ironing, degradation conditions of FC, and different MFCS system distributions are all taken into account to realize the customized power generation plans.

3.1.1. *First-layer energy management system*

The major objective of the first layer is to make the day-ahead energy dispatching plans with the minimized fuel consumption. Therefore, the cost function is formulated based on the daily hydrogen consumption by the MFCS and is described as follows,

$$\min_{P_{fc,i,t}, k_{fc,i,t}} \quad J = \sum_{t=1}^{24} \sum_{i=1}^{N_{fc}} k_{fc,i,t} \times \frac{P_{fc,i,t}}{\eta_{fc,i,t}} \tag{21}$$

where $k_{fc,i,t}$ stands for the on/off of ith FC at time t. $P_{fc,i,t}$ is the output power of it, and $\eta_{fc,i,t}$ is the corresponding efficiency, which can be obtained by the look-up table from Section 2.

The cost function is subject to different constraints when the ship is on sail and when it is at the port. When the ship is on sail, the load demand is supported all by the FCs and battery. So the constraints are as follows,

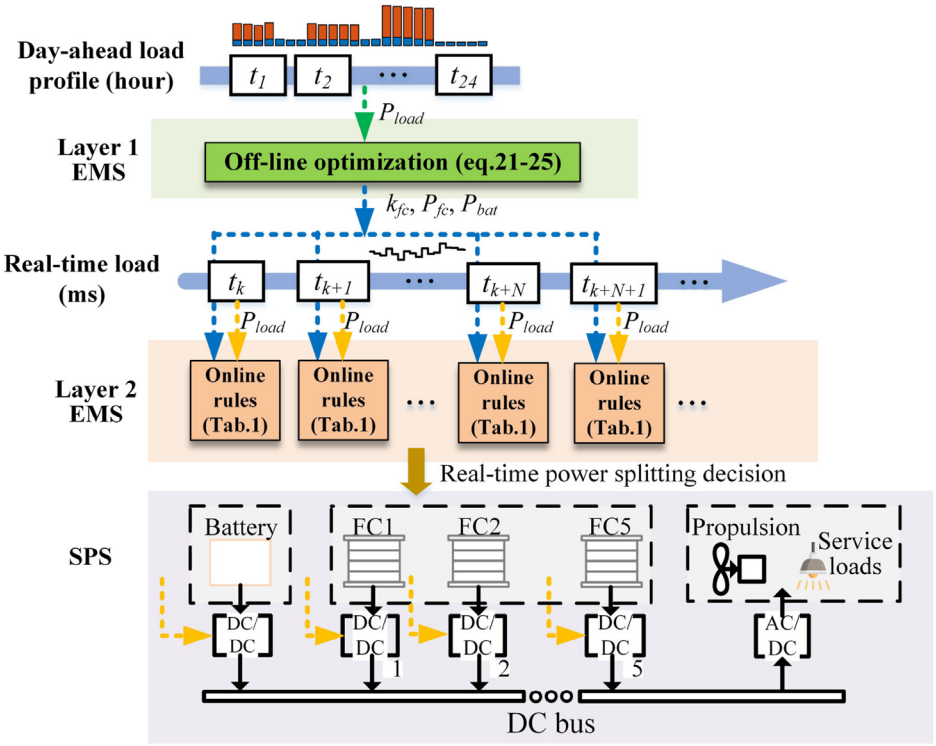

Fig. 4 – The proposed two-layer EMS scheme for the shipboard microgrid.

$$\begin{aligned}
&C_{s1}: \sum_{i=1}^{N_{fc}} k_{fc,i,t} P_{fc,i,t} + P_{bat,t} = P_{load,t} \\
&C_{s2}: k_{fc,i,t} \in \{0,1\} \\
&C_{s3}: P_{fc,i,t} \in [P_{fc(min)},\ P_{fc(max)}] \\
&C_{s4}: P_{bat,t} \in [P_{bat(min)},\ P_{bat(max)}] \\
&C_{s5}: SOC_{bat,t} \in [SOC_{bat(min)}, SOC_{bat(max)}]
\end{aligned} \tag{22}$$

The equality constraints ensures the power balance. $P_{fc(min)}$, $P_{fc(max)}$, $P_{bat(min)}$, $P_{bat(max)}$, $SOC_{bat(min)}$, and $SOC_{bat(max)}$ are the lower and upper limits of the FC output power, battery output power, and battery SOC, respectively. When the ship arrives at the port, it gets access to the cold-ironing power ($P_{ci,t}$). So the constraints are as follows,

$$\begin{aligned}
&C_{p1}: \sum_{i=1}^{N_{fc}} k_{fc,i,t} P_{fc,i,t} + P_{bat,t} + P_{ci,t} = P_{load,t} \\
&C_{p2}: k_{fc,i,t} \in \{0,1\} \\
&C_{p3}: P_{fc,i,t} \in [P_{fc(min)}, P_{fc(max)}] \\
&C_{p4}: P_{bat,t} \in [P_{bat(min)}, P_{bat(max)}] \\
&C_{p5}: SOC_{bat,t} \in [SOC_{bat(min)}, SOC_{bat(max)}] \\
&C_{p6}: SOC_{bat,24} \geq 0.6
\end{aligned} \tag{23}$$

C_{p6} restrains the final state of battery SOC. In order to guarantee sufficient energy backup for the future voyages, SOC_{bat} is set to be greater than 0.6 at the end of the day.

Changes in ship cruising plan would have direct effects on the load profile, which is represented by $P_{load,t}$. Changes in the FC degradation levels would affect the efficiency curve and is reflected by $\eta_{fc,i,t}$. Different ways of power distribution among MFCS system add additional constraints to the optimization problem as follows:

1. For equal distribution, the power demand is equally allocated to each FC stack, therefore the on/off signal and output power for each FC is the same. So the following constraints are held additionally for ships on sail and at port.

$$\begin{aligned}
&C_{equ.1}: k_{fc,i,t} = k_{fc,j,t} \quad \forall i,j \in \mathbb{N}_{fc} \\
&C_{equ.2}: P_{fc,i,t} = P_{fc,j,t} \quad \forall i,j \in \mathbb{N}_{fc}
\end{aligned} \tag{24}$$

2. For sequential distribution, the next FC runs only when the former FC reaches its maximum output power. And the additional constraints in this case is presented by,

$$C_{seq.1}: k_{fc,i+1,t} = \begin{cases} 0 & P_{fc,i,t} k_{fc,i,t} < P_{fc(max)} \\ 1 & P_{fc,i,t} k_{fc,i,t} = P_{fc(max)} \end{cases} \tag{25}$$

3. For independent distribution, no extra constraints are required since each FC runs independently.

3.1.2. *Second-layer PMS*

Based on the day-ahead energy dispatching decision, the second layer decides the real-time power splitting using the previous decisions as reference. This layer consists of 5 states for the possible operating cases and requires information of battery SOC (SOC_{bat}), real-time load information (P_{load}), and hourly MFCS output power ($P_{tot,ref}$) from the first layer as shown in Table 1. The on/off status of each FC stack is decided by the first layer and the output power of them follows the state-based rules. Then, the difference between the required load demand and the output power of MFCS system is

supported by the battery. The overall idea is to discharge the battery at high SOC conditions, and to charge the battery at low SOC, thus ensuring a healthy level of SOC throughout the cruise.

3.2. Other energy management strategies

In order to evaluate the effectiveness of the proposed EMS, the previously commonly adopted EMSs that are suitable for real-time application are described and compared.

3.2.1. Equivalent consumption minimization strategy

Equivalent consumption minimization strategy (ECMS) is one of the most commonly adopted optimization-based methods that has been widely used on real-time power splitting problems, and is considered to have the near-optimal solution [61]. The overall idea of EMCS is to consider the battery as an energy buffer and assumes that all the energy discharged from the battery will eventually be charged back later [62]. It offers a way to calculate the equivalent fuel consumption of the battery. Based on this concept, an ECMS-based optimization algorithm is developed for the studied shipboard microgrid, which is formulated as:

$$\min J = \sum_{i=1}^{N_{fc}} \dot{C}_{fc,i} + \dot{C}_{bat} \tag{26}$$

$$\begin{aligned} &C_1 : \textstyle\sum_{i=1}^{N_{fc}} P_{fc,i} \times k_{fc,i} + P_{bat} = P_{load} \\ &C_2 : P_{fc,i} \in [P_{fc(min)}, P_{fc(max)}] \\ &C_3 : I_{bat} \in [I_{bat(min)}, I_{bat(max)}] \\ &C_4 : SOC_{bat} \in [SOC_{bat(min)}, SOC_{bat(max)}] \\ &C_5 : u_{fc} \in [P_{fc.i,ref} - \Delta P_{fc}, P_{fc.i,ref} + \Delta P_{fc}] \\ &C_6 : \Delta u_{fc,i} \le \Delta u_{fc(max)} \end{aligned} \tag{27}$$

where $\dot{C}_{fc,i}$ is the instantaneous fuel consumption rate of single FC, which can be calculated by Equation (16). $P_{fc,i,ref}$ is the reference FC output value from the upper layer, and ΔP_{fc} is the allowed variation from the reference value and is set as 30 kW in the following case studies. $\dot{C}_{bat}$ is the equivalent instantaneous fuel consumption rate of battery, and is calculated as follows,

$$\dot{C}_{bat} = ef_{bat} \frac{P_{bat}}{\eta_{fc.av} LHV_{fuel}} \tag{28}$$

where $\eta_{fc.av}$ is the average efficiency of fuel cell. ef_{bat} is the equivalence factor that represents the conversion from electricity to hydrogen consumption and is calculated by the following equations [63],

$$ef_{bat} = \begin{cases} \dfrac{k_{bat}}{\eta_{chg.av} \cdot \eta_{dis}} & P_{bat} \ge 0 \\ k_{bat} \cdot \eta_{dis.av} \cdot \eta_{chg} & P_{bat} < 0 \end{cases} \tag{29}$$

where $\eta_{chg.av}$ and $\eta_{dis.av}$ are the average charging and discharging efficiency of battery. η_{chg} and η_{dis} are the real-time battery charging and discharging efficiencies and are calculated based on [64]. k_{bat} denotes the SOC penalty coefficient, which, after proper design, can help maintain the battery SOC around a healthy level. In this paper, it is defined as:

Table 1 – Second-layer rule-based PMS.

SOC_{bat}	State	Load	MFCS power ($u_{fc,tot}$)
$SOC_{bat} > 0.8$	1	$P_{load} \ge P_{tot,ref}$	$P_{tot,ref}$
	2	$P_{load} < P_{tot,ref}$	P_{load}
$0.5 \le SOC_{bat} \le 0.8$	3	$P_{load} \le P_{tot,ref}$	$P_{tot,ref}$
	4	$P_{load} > P_{tot,ref}$	$P_{tot,ref}$
$SOC_{bat} < 0.5$	5	$P_{load} \ge P_{tot,ref}$	P_{load}
	6	$P_{load} < P_{tot,ref}$	$P_{tot,ref}$

$$k_{bat} = 1 - \mu_{bat} \frac{SOC_{bat} - SOC_{desire}}{SOC_{desire}} \tag{30}$$

Here μ_{bat} stands for the penalty of SOC when it violates the desired value (SOC_{desire}). k_{bat} varies with SOC and therefore ensures that the battery stays around the desired SOC level.

3.2.2. State-based method

Rule-based method has been widely adopted in the existing literature for real-time power splitting due to its advantages in simple structure and fast computing speed. Here in this paper, a state-based power management strategies developed based on [31] is taken as an example to evaluate the performance of the proposed EMS and is presented in Table 2. $P_{fc.tot(min)}$, $P_{fc.tot(max)}$ are the minimum and maximum power limits for the MFCS system. P_{optdis}, $P_{optchar}$ are the optimal discharge and charge power for the battery.

4. Case studies

Table 3 gives the parameters of the on-board electrical facilities of the studied ships. To evaluate the performance of the proposed EMS in day-ahead energy dispatching and real-time power splitting, several case studies are conducted. The two layers operate on different time scales. The first layer uses a sampling time of 1 h, while the second layer employs a sampling time of 0.1 s. And the state-based and ECMS-based methods (as has been discussed in Section 3) are adopted to benchmark the performance of the proposed EMS in terms of power splitting, SOC conditions, and fuel savings. These case studies are conducted in GAMS and MATLAB/Simulink 2022a, where the former software was used for the optimization and the latter for the dynamic modelling.

Table 2 – State-based PMS.

SOC_{bat}	State	Load	MFCS power
$SOC_{bat} > 0.8$	1	$P_{load} \le P_{fc.tot(min)}$	off
	2	$P_{load} \le P_{fc.tot(min)} + P_{optdis}$	$P_{fc.tot(min)}$
	3	$P_{load} \le P_{fc.tot(max)} + P_{optdis}$	$P_{load} - P_{optdis}$
	4	$P_{load} > P_{fc.tot(max)} + P_{optdis}$	$P_{fc.tot(max)}$
$0.5 \le SOC_{bat} \le 0.8$	5	$P_{load} \le P_{fc.tot(min)}$	$P_{fc.tot(min)}$
	6	$P_{load} \le P_{fc.tot(max)}$	P_{load}
	7	$P_{load} > P_{fc.tot(max)}$	$P_{fc.tot(max)}$
$SOC_{bat} < 0.5$	8	$P_{load} \le P_{fc.tot(max)} - P_{optchar}$	$P_{load} + P_{optchar}$
	9	$P_{load} > P_{fc.tot(max)} - P_{optchar}$	$P_{fc.tot(max)}$

Table 3 – Electrical parameters for SPS.

Equipment	Parameters	Symbol	Values
FC module	Number of FC modules	N_{fc}	5
	Maximum output power	$P_{fc(max)}$	200 kW
	Minimum output power	$P_{fc(min)}$	15 kW
Battery	Quantities	N_{bat}	20
	Capacity	Q_{bat}	200 Ah
	Voltage	V_{oc}	125V
	SOC limits	$SOC_{bat(min)}$, $SOC_{bat(max)}$	0.3,0.95
	Desired SOC level	SOC_{desire}	0.6
	Initial SOC	SOC_{init}	0.6
	Optimal discharging power	P_{optdis}	20 kW
	Optimal charging power	$P_{optchar}$	15 kW

4.1. *Day-ahead energy generation plans*

To test the feasibility of the proposed strategy in different conditions, multiple case studies are performed under four FC distributions (equal, independent, sequential, and rotational sequential), three different cruises (Cruise 1, Cruise 2, and Cruise 3), and five MFCS degradation cases (as in Table 4).

The cruise schedule for Cruise 1 is depicted in Fig. 5a. The ferry leaves from Port A at 6:00 and reaches Port B at 9:00. Following a 3-h docking period, the ferry sets sail from Port B at 13:00, arriving at Port C at 17:00. Subsequently, the vessel departs for Port A at 20:00, with an estimated arrival time of 00:00. It is assumed that the vessel gets access to the cold ironing during its stay at the ports. In Cruise 2, the availability of cold-ironing in Port C is disrupted due to maintenance. Despite this, the ferry follows a similar routine to Cruise 1. In Cruise 3, the ferry operates exclusively between Port A and Port C, as illustrated in Fig. 5b. It departs from Port A at 9:00 and reaches Port C at 13:00. Following a 6-h docking period, the ferry sets sail once again at 20:00, returning to Port A by 00:00.

The system performance under each cruises and four different degradation cases can be found in Appendix A. Taking the ship in Cruise 1 with FC degradation statue as Case 4 as an example, results are presented in Fig. 6 in regards to power sharing, load tracking, and battery SOC. During times 1–4, 8–12, and 15–19, the ship is at sea and the fuel cells provide the primary power supply. During times 5–8, 13, 14, and 20–24, the ship arrives at the harbors, and cold-ironing supports the service load while charging the batteries. Power sharing among the fuel cells varies under different MFCS distribution ways, but the load requirements are all satisfactorily met, and the battery SOC levels are maintained at healthy levels throughout the voyage. Moreover, as FC1, FC2, and FC3 degrades more than the others, the independent and rotational sequential distributions facilitate more efficient operation by distributing more power to the more healthy ones, i.e. FC4 and FC5.

Table 4 – Five degradation cases of MFCS (BoL: undegraded, 10k: after 10 k hours usage, 20k: after 20 k hours usage, 30k: after 30 k hours usage).

	FC1	FC2	FC3	FC4	FC5
Case 1	BoL	BoL	BoL	BoL	BoL
Case 2	10k	BoL	BoL	BoL	BoL
Case 3	20k	10k	BoL	BoL	BoL
Case 4	30k	20k	10k	BoL	BoL
Case 5	30k	20k	10k	10k	BoL

Fig. 7a presents the fuel consumption results under each circumstances. State-based method as discussed in Section 3.2.2 is used as a benchmark and is tested for equal, sequential, and rotational sequential distributions under each cruising and degrading cases, respectively. Due to the reason that independent distribution must rely on optimization for power allocation, state-based method is not applicable.

Based on the comprehensive results presented in Appendix A, it is obvious that the fuel cells serve as the primary power source during the vessel's operations at sea, and the cold ironing supports the service load and charges the batteries when arrives at ports. In addition to that, several observations have been made and are presented below:

1. The proposed EMS outperforms the state-based method, achieving up to 7.13% improvement in fuel savings with the same fuel cell distribution. Furthermore, when compared to independent distribution, the fuel savings improvement can reach up to 28%.
2. As fuel cells degrade, their efficiency decreases. Among different distribution strategies, independent distribution and rotational sequential distribution demonstrate better fuel efficiency under highly degraded conditions compared to other approaches. Independent distribution exhibits the lowest fuel consumption due to its high flexibility. On the other hand, sequential distribution, particularly under highly degraded conditions, consumes the most fuel. However, by incorporating the rotation mode, the rotational sequential distribution achieves significant fuel savings, improving efficiency by up to 23.2% compared to traditional sequential distribution alone.
3. Through the proposed day-ahead EMS, it is observed that the battery SOC remains within a healthy range of 30%–95% throughout the full-day cruising. Moreover, the SOC reaches a high level (higher than 60%) at the end of the voyage, indicating promising energy reserves for future cruises.

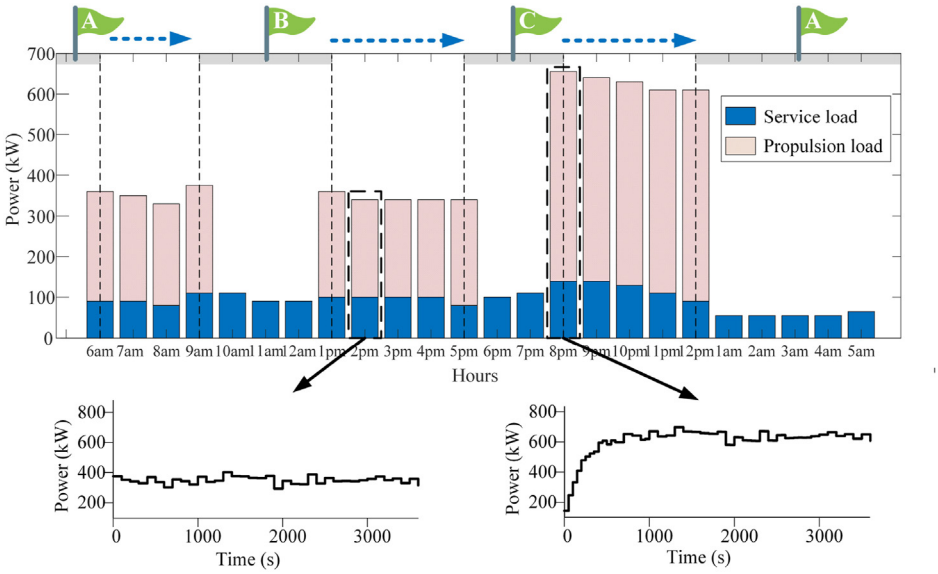

(a) Cruise 1 and Cruise 2

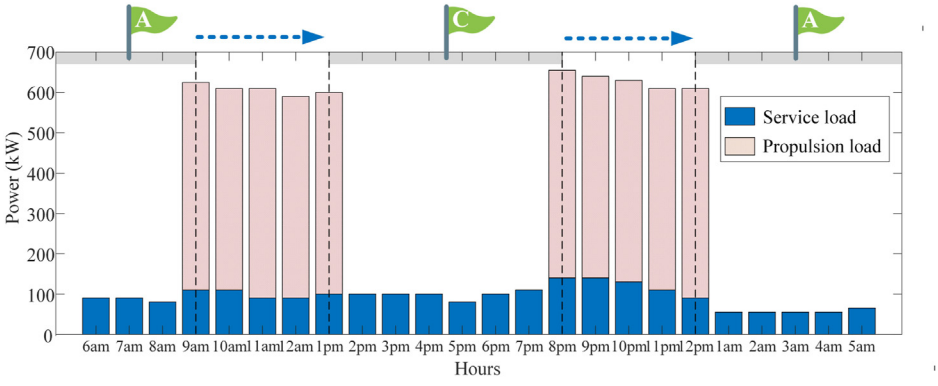

(b) Cruise 3

Fig. 5 – Ferry routine and load profile under three cruises.

4.2. *Real-time power splitting*

As has been verified in Section 4.1, the first-layer EMS gives a 24-h power generation plan based on the hourly average load profile. However, due to the highly dynamic load demands, the results are not directly applied to real time, but provide references for the second-layer PMS for instantaneous power splitting. In order to evaluate the performance of the proposed EMS, case studies are conducted under moderate and extreme real-time load conditions, respectively. And ECMS-based method is adopted as a benchmark due to its advantages in solving the real-time power allocation problem for multi-energy system with near-optimal solutions.

The case study under moderate load is tested at 14:00–15:00 under cruise 1, when the ship is cruising at a fixed low speed. As shown in Fig. 5a, the average hourly load demand at that time is 340 kW, but the real-time load fluctuates occasionally due to variations in service load demand. The extreme case study is conducted under Cruise 1 during 20:00–21:00 when the ship is leaving Port C and towards Port A with full speed. The average load demand at that time is 655 kW, but the real-time load varies significantly between 110 kW and 700 kW during the first 25 min due to the acceleration of the ship. All the case studies are performed with FCs in different degradation status as case 4 in Table 4.

The simulation results of real-time ship performance in the case of extreme condition is given in Fig. 8 as an example. It can be concluded that the two approaches, while distributing power differently, both ensure stable operation and healthy SOC levels under highly variable load conditions. Fig. 7b gives the fuel consumption results for the two methods during the time periods 14:00–15:00 and 20:00–21:00, respectively. And Table 5 gives the required

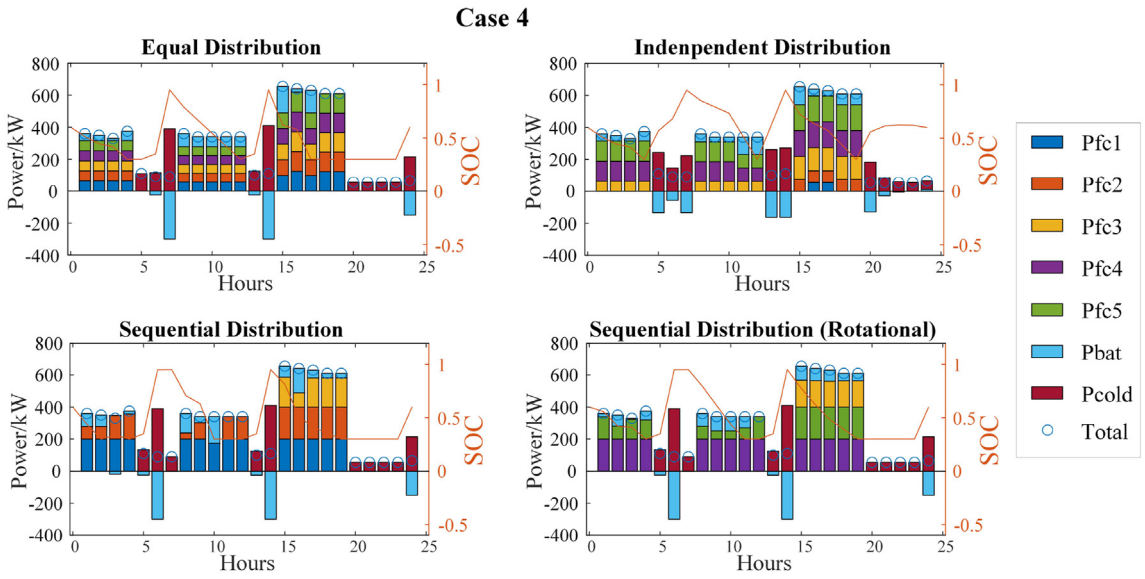

Fig. 6 – System performance in Cruise 1 under degradation Case 4.

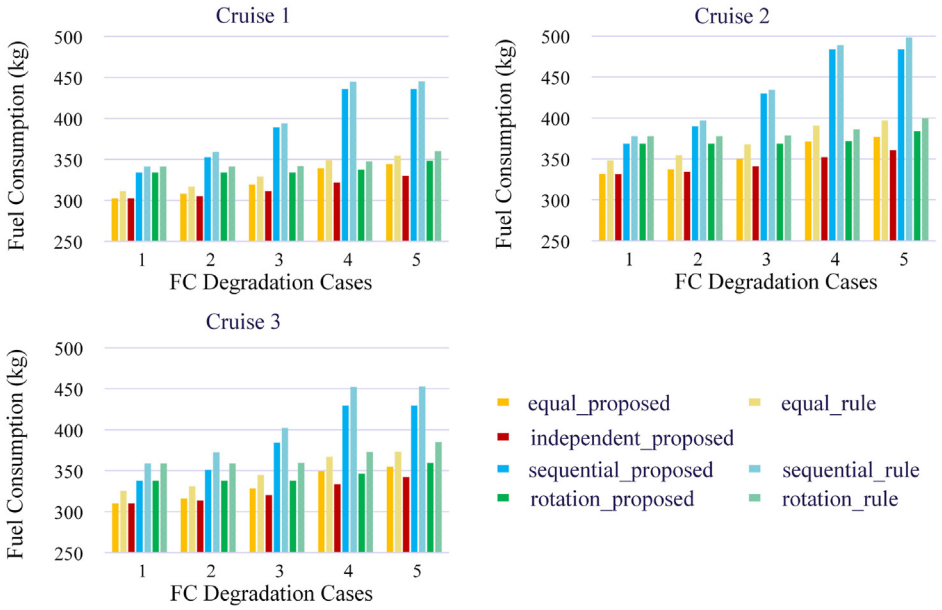

(a) Daily fuel consumption results comparison

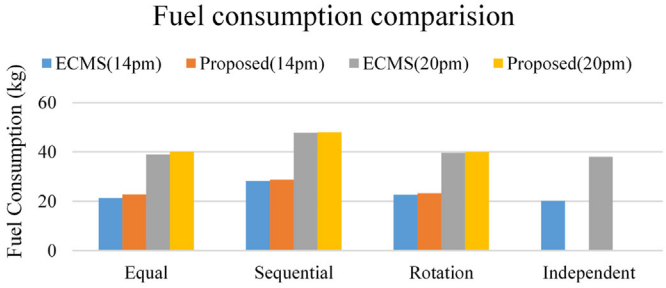

(b) Hourly fuel consumption results comparison

Fig. 7 – Fuel consumption comparisons.

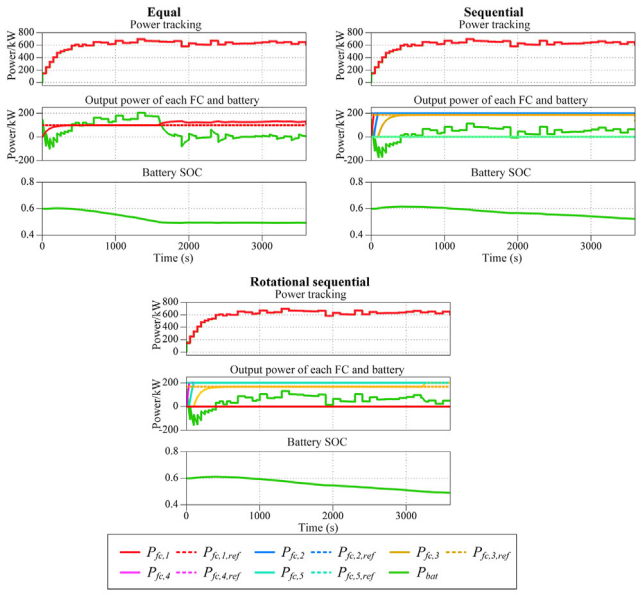

(a) Performance under the proposed method

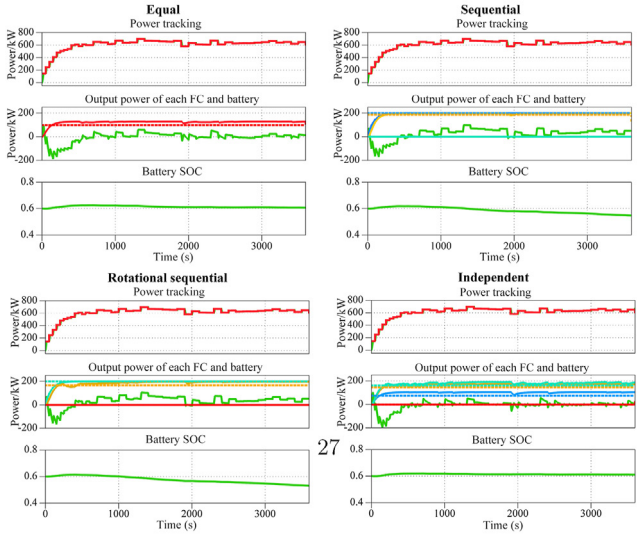

(b) Performance under the ECMS-based method

Fig. 8 – Ship performance during an 1-h cruise.

computation time for both methods. It can be concluded that the ECMS has the best fuel economy for all FC distributions, but it requires much longer calculation time. The proposed method, on the other hand, achieves almost as good performance as the ECMS (101%–106% compared to the ECMS value), but saves 99.9% of the computation time. In addition, the difference of fuel consumption between the proposed method and the ECMS-based method decreases under extreme load conditions (maximum 3.48% decrease), indicating that the proposed method shows better robustness under highly variable conditions.

Further more, among the four MFCS distributions, the rotational sequential distribution is highly recommended because of its good performance in terms of fuel savings (almost as good as the independent distribution), similar FC degradating rate, and less computational effort.

Table 5 – Computation time required for each sampling interval.

	Equal	Sequential	Rotational	Independent
ECMS	8 ms	10 ms	10 ms	8 ms
Proposed	10μs	4.50μs	6.00μs	–
	Percentage of the time saving for the proposed method			
Proposed	99.87%	99.96%	99.94%	–

5. Conclusion

In order to improve fuel efficiency in the face of variable cruising conditions, this paper presents a two-layer energy management system for the hybrid multi-PEM fuel cell stack/battery passenger ship. The developed first-layer EMS is optimization-based and is capable of customizing the power generation plan based on different cruising, FC degradation, and distribution conditions. The second-layer PMS is rule-based, which manages to distribute the power with high fuel efficiency and less computational effort. To better evaluate the effectiveness of the proposed method, the ECMS-based method and previously adopted state-based method are used as benchmarks.

Compared to the previous work, this paper fully investigates the distinct attributes of onboard load and fuel cell dynamics. The constructed PMS is built with fully consideration of the long-term and short-term load features and therefore addresses the needs of achieving globally optimum solutions and coping with real-time applicability. In addition to it, the fuel cells are detailed modeled with consideration of degradation status. And the specific requirements of multi-fuel cell stack systems are fully considered with respects to different electrical distributions.

Multiple case studies show that the proposed method has good performance (high fuel-efficiency power sharing, real-time load tracking, and effective energy reservation) both for offline long-term energy efficiency dispatching and for online real-time application under different cruising conditions. It saves up to 28% of fuel compared to the state-based method and 99.9% computational time compared to the ECMS-based method.

In addition, out of all the distribution ways, the rotational sequential distribution is highly recommended due to its high fuel efficiency, lower computational effort required, and ability to prevent fuel cells from unequally degrading.

However, in this paper, it is assumed that all FC degradation states are known. In future work, the estimation and prediction of FC degradation should be taken into account to enable more practical and precise operation.

Declaration of competing interest

The authors declare that they have no known competing financial interests or personal relationships that could have appeared to influence the work reported in this paper.

Acknowledgement

We would like to acknowledge the project LH2Vessel (EUDP J.Nr. 64019-0023) and the project VILLUM Investigator (Grant 25920) for sponsoring this research.

Appendix A. Supplementary data

Supplementary data to this article can be found online at https://doi.org/10.1016/j.ijhydene.2023.09.297.

REFERENCES

[1] Armellini A, Daniotti S, Pinamonti P, Reini M. Evaluation of gas turbines as alternative energy production systems for a large cruise ship to meet new maritime regulations. Appl Energy 2018;211:306–17.
[2] IMO C. Fourth imo ghg study 2020. 2020.
[3] Bassam AM, Phillips AB, Turnock SR, Wilson PA. Development of a multi-scheme energy management strategy for a hybrid fuel cell driven passenger ship. Int J Hydrogen Energy 2017;42(1):623–35.
[4] Choi M, Kim M, Sohn Y-J, Kim S-G. Development of preheating methodology for a 5 kw ht-pemfc system. Int J Hydrogen Energy 2021;46(74):36982–94.
[5] Wang Y, Sun Z, Chen Z. Energy management strategy for battery/supercapacitor/fuel cell hybrid source vehicles based on finite state machine. Appl Energy 2019;254:113707.
[6] Zhou S, Fan L, Zhang G, Gao J, Lu Y, Zhao P, Wen C, Shi L, Hu Z. A review on proton exchange membrane multi-stack fuel cell systems: architecture, performance, and power management. Appl Energy 2022;310:118555.
[7] Shotorbani AM, Zeinal-Kheiri S, Chhipi-Shrestha G, Mohammadi-Ivatloo B, Sadiq R, Hewage K. Enhanced real-time scheduling algorithm for energy management in a renewable-integrated microgrid. Appl Energy 2021;304:117658.
[8] Navas SJ, González GC, Pino F. Hybrid power-heat microgrid solution using hydrogen as an energy vector for residential houses in Spain. a case study. Energy Convers Manag 2022;263:115724.
[9] Saffar A, Ghasemi A. Energy management of a renewable-based isolated micro-grid by optimal utilization of dump loads and plug-in electric vehicles. J Energy Storage 2021;39:102643.
[10] Lei T, Min Z, Gao Q, Song L, Zhang X, Zhang X. The architecture optimization and energy management technology of aircraft power systems: a review and future trends. Energies 2022;15(11):4109.
[11] Fang S, Xu Y. Multi-objective robust energy management for all-electric shipboard microgrid under uncertain wind and wave. Int J Electr Power Energy Syst 2020;117:105600.
[12] Geertsma R, Negenborn R, Visser K, Hopman J. Design and control of hybrid power and propulsion systems for smart ships: a review of developments. Appl Energy 2017;194:30–54.
[13] Nasiri S, Peyghami S, Parniani M, Blaabjerg F. Power management strategies based on propellers speed control in waves for mitigating power fluctuations of ships. IEEE Transactions on Transportation Electrification 2022;8(3):3247–60.
[14] Dall'Armi C, Pivetta D, Taccani R. Health-conscious optimization of long-term operation for hybrid pemfc ship propulsion systems. Energies 2021;14(13):3813.
[15] Li X, Huang J, Zhang J, Zhou M, Wang T, Tang X, Lai J, Yang X. An adaptive multi-objective joint optimization framework for marine hybrid energy storage system design considering energy management strategy. J Energy Storage 2023;68:107689.
[16] Hein K, Murali R, Xu Y, Aditya V, Gupta AK. Battery thermal performance oriented all-electric ship microgrid modeling, operation and energy management scheduling. J Energy Storage 2022;48:103970.
[17] Wang Z, Ma Y, Sun Y, Tang H, Cao M, Xia R, Han F. Optimizing energy management and case study of multi-energy coupled supply for green ships. J Mar Sci Eng 2023;11(7):1286.
[18] Wang X, Yuan Y, Tong L, Yuan C, Shen B, Long T. Energy management strategy for diesel–electric hybrid ship considering sailing route division based on ddpg. IEEE Transactions on Transportation Electrification; 2023.
[19] Hein K, Xu Y, Senthilkumar Y, Gary W, Gupta AK. Rule-based operation task-aware energy management for ship power systems, IET Generation. Transm Distrib 2020;14(25):6348–58.
[20] Bukar AL, Tan CW, Yiew LK, Ayop R, Tan W-S. A rule-based energy management scheme for long-term optimal capacity planning of grid-independent microgrid optimized by multi-objective grasshopper optimization algorithm. Energy Convers Manag 2020;221:113161.
[21] Haseltalab A, van Biert L, Sapra H, Mestemaker B, Negenborn RR. Component sizing and energy management for sofc-based ship power systems. Energy Convers Manag 2021;245:114625.
[22] Letafat A, Rafiei M, Sheikh M, Afshari-Igder M, Banaei M, Boudjadar J, Khooban MH. Simultaneous energy management and optimal components sizing of a zero-emission ferry boat. J Energy Storage 2020;28:101215.
[23] Ganjian M, Farahabadi HB, Alirezapouri MA, Firuzjaei MR. Optimal design strategy for fuel cell-based hybrid power system of all-electric ships. Int J Hydrogen Energy 2023. https://doi.org/10.1016/j.ijhydene.2023.07.258.
[24] Perna A, Jannelli E, Di Micco S, Romano F, Minutillo M. Designing, sizing and economic feasibility of a green hydrogen supply chain for maritime transportation. Energy Convers Manag 2023;278:116702.
[25] Si Y, Wang R, Zhang S, Zhou W, Lin A, Zeng G. Configuration optimization and energy management of hybrid energy system for marine using quantum computing. Energy 2022;253:124131.
[26] Jin H, Yang X. Bilevel optimal sizing and operation method of fuel cell/battery hybrid all-electric shipboard microgrid. Mathematics 2023;11(12):2728.
[27] Chen H, Zhang Z, Guan C, Gao H. Optimization of sizing and frequency control in battery/supercapacitor hybrid energy storage system for fuel cell ship. Energy 2020;197:117285.
[28] Kistner L, Bensmann A, Hanke-Rauschenbach R. Optimal design of power gradient limited solid oxide fuel cell systems with hybrid storage support for ship applications. Energy Convers Manag 2021;243:114396.
[29] Azib T, Bethoux O, Remy G, Marchand C, Berthelot É. An innovative control strategy of a single converter for hybrid fuel cell/supercapacitor power source. IEEE Trans Ind Electron 2010;57(12):4024–31.
[30] Bassam AM, Phillips AB, Turnock SR, Wilson PA. An improved energy management strategy for a hybrid fuel cell/battery passenger vessel. Int J Hydrogen Energy 2016;41(47):22453–64.

[31] Han J, Charpentier J-F, Tang T. An energy management system of a fuel cell/battery hybrid boat. Energies 2014;7(5):2799–820.
[32] Lin X, Wang Z, Zeng S, Huang W, Li X. Real-time optimization strategy by using sequence quadratic programming with multivariate nonlinear regression for a fuel cell electric vehicle. Int J Hydrogen Energy 2021;46(24):13240–51.
[33] Fathy A, Rezk H, Nassef AM. Robust hydrogen-consumption-minimization strategy based salp swarm algorithm for energy management of fuel cell/supercapacitor/batteries in highly fluctuated load condition. Renew Energy 2019;139:147–60.
[34] Gao H, Wang Z, Yin S, Lu J, Guo Z, Ma W. Adaptive real-time optimal energy management strategy based on equivalent factors optimization for hybrid fuel cell system. Int J Hydrogen Energy 2021;46(5):4329–38.
[35] Xie P, Tan S, Bazmohammadi N, Guerrero JM, Vasquez JC. A real-time power management strategy for hybrid electrical ships under highly fluctuated propulsion loads. IEEE Syst J 2023;17(1):395–406.
[36] Cavo M, Rivarolo M, Gini L, Magistri L. An advanced control method for fuel cells-metal hydrides thermal management on the first Italian hydrogen propulsion ship. Int J Hydrogen Energy 2023;48(54):20923–34.
[37] Wu P, Partridge J, Bucknall R. Cost-effective reinforcement learning energy management for plug-in hybrid fuel cell and battery ships. Appl Energy 2020;275:115258.
[38] Gaber M, El-Banna S, El-Dabah M, Hamad M. Intelligent energy management system for an all-electric ship based on adaptive neuro-fuzzy inference system. Energy Rep 2021;7:7989–98.
[39] Abdelqawee IM, Emam AW, ElBages MS, Ebrahim MA. An improved energy management strategy for fuel cell/battery/supercapacitor system using a novel hybrid jellyfish/particle swarm/bat optimizers. J Energy Storage 2023;57:106276.
[40] Luna M, La Tona G, Accetta A, Pucci M, Pietra A, Di Piazza MC. Optimal management of battery and fuel cell-based decentralized generation in dc shipboard microgrids. Energies 2023;16(4):1682.
[41] Cheng Y, Zhang Y, Chen Q. Energy management strategy of fuel-cell backup power supply systems based on whale optimization fuzzy control. Electronics 2022;11(15):2325.
[42] Peng X, Chen H, Guan C. Energy management optimization of fuel cell hybrid ship based on particle swarm optimization algorithm. Energies 2023;16(3):1373.
[43] Ma Z, Chen H, Han J, Chen Y, Kuang J, Charpentier J-F, At-Ahmed N, Benbouzid M. Optimal soc control and rule-based energy management strategy for fuel-cell-based hybrid vessel including batteries and supercapacitors. J Mar Sci Eng 2023;11(2):398.
[44] Ferahtia S, Djeroui A, Rezk H, Houari A, Zeghlache S, Machmoum M. Optimal control and implementation of energy management strategy for a dc microgrid. Energy 2022;238:121777.
[45] Xie P, Asgharian H, Vasquez JC, Guerrero J, Araya SS, Liso V. Day-ahead energy management for hybrid electric vessel with different pem fuel cell modular configurations. Energy Rep 2023;9:99–106.
[46] Jian B, Wang H. Hardware-in-the-loop real-time validation of fuel cell electric vehicle power system based on multi-stack fuel cell construction. J Clean Prod 2022;331:129807.
[47] Liso V, Xie P, Araya SS, Guerrero JM. Modelling a modular configuration of pem fuel cell system for vessels applications. In: 7TH world maritime technology conference 2022; 2022.
[48] Garcia JE, Herrera DF, Boulon L, Sicard P, Hernandez A. Power sharing for efficiency optimisation into a multi fuel cell system. In: 2014 IEEE 23rd international symposium on industrial electronics (ISIE). IEEE; 2014. p. 218–23.
[49] Macias A, Kandidayeni M, Boulon L, Chaoui H. A novel online energy management strategy for multi fuel cell systems. In: 2018 IEEE international conference on industrial technology (ICIT). IEEE; 2018. p. 2043–8.
[50] Han X, Li F, Zhang T, Zhang T, Song K. Economic energy management strategy design and simulation for a dual-stack fuel cell electric vehicle. Int J Hydrogen Energy 2017;42(16):11584–95.
[51] Fernandez AM, Kandidayeni M, Boulon L, Chaoui H. An adaptive state machine based energy management strategy for a multi-stack fuel cell hybrid electric vehicle. IEEE Trans Veh Technol 2019;69(1):220–34.
[52] Macias A, Kandidayeni M, Boulon L, Chaoui H. A novel online energy management strategy for multi fuel cell systems. In: 2018 IEEE international conference on industrial technology (ICIT). IEEE; 2018. p. 2043–8.
[53] Han Y, Li Q, Wang T, Chen W, Ma L. Multisource coordination energy management strategy based on soc consensus for a pemfc–battery–supercapacitor hybrid tramway. IEEE Trans Veh Technol 2017;67(1):296–305.
[54] Rafiei M, Boudjadar J, Khooban M-H. Energy management of a zero-emission ferry boat with a fuel-cell-based hybrid energy system: feasibility assessment. IEEE Trans Ind Electron 2020;68(2):1739–48.
[55] Vásquez CAM. Evaluation of medium speed diesel generator sets and energy storage technologies as alternatives for reducing fuel consumption and exhaust emissions in electric propulsion systems for psvs. Ciencia y tecnología de buques 2016;9(18):49–62.
[56] Dutta S, Shimpalee S, Van Zee J. Numerical prediction of mass-exchange between cathode and anode channels in a pem fuel cell. Int J Heat Mass Tran 2001;44(11):2029–42.
[57] Pei P, Ouyang M, Feng W, Lu L, Huang H, Zhang J. Hydrogen pressure drop characteristics in a fuel cell stack. Int J Hydrogen Energy 2006;31(3):371–7.
[58] Liso V, Nielsen MP, Kær SK, Mortensen HH. Thermal modeling and temperature control of a pem fuel cell system for forklift applications. Int J Hydrogen Energy 2014;39(16):8410–20.
[59] My engineering tools. https://myengineeringtools.com/Compressors/Tools_Compressor_Power.html.
[60] Chen H, Pei P, Song M. Lifetime prediction and the economic lifetime of proton exchange membrane fuel cells. Appl Energy 2015;142:154–63.
[61] Xie P, Guerrero JM, Tan S, Bazmohammadi N, Vasquez JC, Mehrzadi M, et al. Optimization-based power and energy management system in shipboard microgrid: a review. IEEE Syst J 2022;16(1):578–90.
[62] Xie P, Tan S, Bazmohammadi N, Guerrero JM, Vasquez JC, Alcala JM, Carreño JEM. A distributed real-time power management scheme for shipboard zonal multi-microgrid system. Appl Energy 2022;317:119072.
[63] Xie P, Tan S, Guerrero JM, Vasquez JC. Mpc-informed ecms based real-time power management strategy for hybrid electric ship. Energy Rep 2021;7:126–33.
[64] Hong Z, Li Q, Han Y, Shang W, Zhu Y, Chen W. An energy management strategy based on dynamic power factor for fuel cell/battery hybrid locomotive. Int J Hydrogen Energy 2018;43(6):3261–72.